

# Transient quantum evolution of 2D electrons under photoexcitation of a deep center

F.T. Vasko\*

*Institute of Semiconductor Physics, NAS Ukraine, Pr. Nauki 41, Kiev, 03028, Ukraine*

A. Hernandez-Cabrera<sup>†</sup> and P. Aceituno

*Dpto. Fisica Basica, Universidad de La Laguna, La Laguna, 38206-Tenerife, Spain*

(Dated: October 25, 2018)

We have considered the ballistic propagation of the 2D electron Wigner distribution, which is excited by an ultrashort optical pulse from a short-range impurity into the first quantized subband of a selectively-doped heterostructure with high mobility. Transient ionization of a deep local state into a continuum conduction  $c$ -band state is described. Since the quantum nature of the photoexcitation, the Wigner distribution over 2D plane appears to be an alternating-sign function. Due to a negative contribution to the Wigner function, the mean values (concentration, energy, and flow) demonstrate an oscillating transient evolution in contrast to the diffusive classical regime of propagation.

PACS numbers: 05.30.-d; 73.20.-r; 78.47.+p

## I. INTRODUCTION

In recent decades, intensive efforts were paid in order to study the quantum coherent properties of different physical systems [1]. During the development of the ultrafast spectroscopy of bulk semiconductors and heterostructures [2], both coherent oscillations between coupled states and different relaxation processes have been investigated (see references in [3] and [4]). Some quantum peculiarities, e.g. in the transport of mesoscopic devices [5] or in the dynamics of electron excited at metallic surfaces [6], were discussed recently but, to the best of our knowledge, the coherent dynamics of a free quasiparticle, which propagates over continuum states, was not measured directly in any solid state system. The quantum response, such as the formation of quasiparticles in different systems [7, 8, 9, 10], has been observed for sub-picosecond stage of evolution. Under theoretical consideration of such kind of measurements (e.g., see [11] and references therein), one can model the photogeneration process using a simple initial condition describing the creation of carriers during a femtosecond temporal interval. At the same time, in the case of photoexcitation of carriers with low concentration and with energy values below the optical phonon energy, the dynamical regime of the response appears to be valid up to nanosecond time interval. It is because both the fast relaxation, due to optical phonon emission, and the carrier-carrier interaction are suppressed. Thus, a possibility is to study the quantum nature of the ballistic transient evolution, caused by the non-classical character of photoexcitation [4, 12].

Modern high-mobility heterostructures are characterized by a momentum relaxation time correspondent to the subnanosecond scale at low temperatures [13]. So that the mean free path appears to be macroscopic ( $>100$

$\mu\text{m}$  if electron energy is about few meV). The photoexcitation of a single deep impurity under a laser pumping focused up to submicron scale [14] can be carried out in a non-doped heterostructure with a low surface concentration of centers (deep centers in bulk GaAs are under consideration since the starting of 70s [15]). Below we consider the transient photoexcitation of electrons from a deep impurity level and the quantum ballistic evolution of the Wigner distribution in the 2D plane over submillimeter distances during nanosecond time interval.

In contrast to transitions between local states, when the Rabi effect (oscillations of population versus pumping intensity [4, 12]) takes place, the level population of a local state under ultrafast photoionization decreases monotonically with the pumping intensity because the excited electron appears to be delocalized over the conduction  $c$ -band. Another peculiarity of the process under consideration is the quantum character of the transient evolution. Due to this, the concentration distribution, which decreases from the center, involves an oscillating contribution and regions of a *negative Wigner distribution* take place. Such a distribution should be considered with the use of the quantum kinetic equation, written in the Wigner representation, due to the following reasons: (a) the energy conservation law is not valid during the photoexcitation process and (b) there is no momentum restrictions on the excited distribution due to the short-range impurity state involved in the phototransition.

In this paper, we restrict ourself to the local time approximation which corresponds to the photoionization above the  $c$ -band edge ( $\Delta\omega\tau_{ex} > 1$ , where  $\Delta\omega$  is the detuning frequency and  $\tau_{ex}$  is the duration of photoexcitation), when only the point (b) is essential. Due to this reason, the mean values (concentration, energy, and flow) show an oscillating behavior in contrast to the diffusive classical regime. Moreover, although the concentration and energy distributions are positive-definite functions, the flow distribution appears to be an alternating-sign one, i.e. a flow may be directed opposite to a concentration gradient. The peculiarities discussed can be veri-

---

\*Electronic address: ftvasko@yahoo.com

<sup>†</sup>Electronic address: ajhernan@ull.es

fied by the use of optical methods or scanning tunneling microscopy, if the measurements can be performed with submicron and subnanosecond resolutions.

The present work is organized as follows. The photoexcitation process, including the evolution of the deep center population and the transient Wigner distribution over  $c$ -band, is described in Sec. II. Section III presents temporal dependencies of the above-introduced functions. The transient dynamics of the mean values is described in Sec. IV. A list of the assumptions used and the discussion of the methods for experimental verification of the peculiarities discussed are given in the concluding section. Appendix contains the description of the classical regime of transient evolution.

## II. ULTRAFAST PHOTOEXCITATION

Under photoexcitation of electrons, transitions from a deep local level into the first subband of  $c$ -band is described by the density matrix of the  $j$ -state,  $\hat{\rho}_{jt}$ . Performing the averaging over the period of the radiation  $\mathbf{E}_t \exp(-i\omega t) + c.c.$  one obtains the quantum kinetic equation [12]:

$$\frac{\partial \hat{\rho}_{jt}}{\partial t} + \frac{i}{\hbar} [\hat{h}_j, \hat{\rho}_{jt}] = \hat{G}_{jt} \quad (1)$$

with the generation rate ( $j \neq j'$ )

$$\begin{aligned} \hat{G}_{jt} &= \left(\frac{e}{\hbar\omega}\right)^2 \int_{-\infty}^t dt' e^{-i\omega(t'-t)} \\ &\times \left\{ \hat{S}_{jt'-t}^+ (\mathbf{E}_{t'} \cdot \hat{\mathbf{v}})_{jj'} \hat{\rho}_{j't'} \hat{S}_{j't'-t} (\mathbf{E}_t \cdot \hat{\mathbf{v}}^+)_{j'j} \right. \\ &+ \left. (\mathbf{E}_t \cdot \hat{\mathbf{v}}^+)_{jj'} \hat{S}_{j't'-t}^+ \hat{\rho}_{j't'} (\mathbf{E}_{t'} \cdot \hat{\mathbf{v}})_{j'j} \hat{S}_{j't'-t} \right\}_{j \neq j'} + H.c.. \end{aligned} \quad (2)$$

Here  $\hat{h}_j$  is the Hamiltonian of the 2D state in the  $c$ -band ( $j = c$ ) or of the state at short-range centre ( $j = h$ ),  $\hat{S}_{j't'-t} = \exp[-i\hat{h}_j(t'-t)/\hbar]$  is the evolution operator of the  $j$ -th state, and  $(\hat{\mathbf{v}})_{jj'}$  is the velocity matrix element for  $j \leftrightarrow j'$  transitions. For the case of a deep center connected to the valence  $v$ -band [16], we use in (2) the interband matrix element of velocity,  $v_{cv}$ , multiplied by the overlap integral between the plane wave of momentum  $\mathbf{p}$  and the local state,  $I_{\mathbf{p}} = \langle \mathbf{p} | h \rangle$ . The evolution of the distribution function over  $c$ -band,  $f_{\mathbf{p}_1 \mathbf{p}_2 t} = \langle \mathbf{p}_1 | \hat{\rho}_{ct} | \mathbf{p}_2 \rangle$ , is governed by the equation:

$$\begin{aligned} \frac{\partial f_{\mathbf{p}_1 \mathbf{p}_2 t}}{\partial t} + \frac{i}{\hbar} (\varepsilon_{p_1} - \varepsilon_{p_2}) f_{\mathbf{p}_1 \mathbf{p}_2 t} &= G_{\mathbf{p}_1 \mathbf{p}_2 t}, \\ G_{\mathbf{p}_1 \mathbf{p}_2 t} &\simeq \left(\frac{eE v_{cv}}{\hbar\omega}\right)^2 I_{\mathbf{p}_1} I_{\mathbf{p}_2}^* w_t \int_{-\infty}^t dt' w_{t'} \\ &\times e^{i(\varepsilon_p/\hbar - \Delta\omega)(t'-t)} n_{t'} + (c.c., \mathbf{p}_1 \longleftrightarrow \mathbf{p}_2) \end{aligned} \quad (3)$$

with the right-hand side dependent on the population of the local state,  $n_t \equiv \langle h | \hat{\rho}_{ht} | h \rangle$ . The generation rate,  $G_{\mathbf{p}_1 \mathbf{p}_2 t}$ , is determined through the 2D kinetic energy

$\varepsilon_p = p^2/m$  with the effective mass of  $c$ -band,  $m$ , the form-factor  $w_t$  introduced by the relation  $\mathbf{E}_t = \mathbf{E} w_t$ , and the detuning energy  $\hbar\Delta\omega$ , which takes into account the subband quantization.

We are using the initial conditions  $f_{\mathbf{p}_1 \mathbf{p}_2 t \rightarrow -\infty} = 0$  and  $n_{t \rightarrow -\infty} = 1$ , which correspond to the single-electron population of the spin-degenerated level, so that the normalization condition takes the form:  $n_t + 2 \sum_{\mathbf{p}} f_{\mathbf{p}, \mathbf{p}t} = 1$ . Evolution of the local state population is governed by the integro-differential equation

$$\begin{aligned} \frac{dn_t}{dt} + 2 \left(\frac{eE v_{cv}}{\hbar\omega}\right)^2 w_t \int_{-\infty}^t dt' w_{t'} n_{t'} \\ \times \sum_{\mathbf{p}} |I_{\mathbf{p}}|^2 \cos\left(\frac{\varepsilon_p}{\hbar} - \Delta\omega\right) (t - t') = 0, \end{aligned} \quad (4)$$

which is obtained from Eqs. (1, 2). Instead of Eq. (3), one can describe the transient evolution of the  $c$ -band distribution through the Wigner function,  $f_{\mathbf{p}, \mathbf{q}t} \equiv f_{\mathbf{p} - \hbar\mathbf{q}/2, \mathbf{p} + \hbar\mathbf{q}/2t}$  which is governed by the equation

$$\left(\frac{\partial}{\partial t} + i\mathbf{q} \cdot \mathbf{v}\right) f_{\mathbf{p}, \mathbf{q}t} = G_{\mathbf{p}, \mathbf{q}t}, \quad (5)$$

with the velocity  $\mathbf{v} = \mathbf{p}/m$ . Similarly, the generation rate,  $G_{\mathbf{p}, \mathbf{q}t} \equiv G_{\mathbf{p} - \hbar\mathbf{q}/2, \mathbf{p} + \hbar\mathbf{q}/2t}$ , is transformed into

$$\begin{aligned} G_{\mathbf{p}, \mathbf{q}t} &\simeq \left(\frac{eE v_{cv}}{\hbar\omega}\right)^2 I_{\mathbf{p} + \frac{\hbar\mathbf{q}}{2}} I_{\mathbf{p} - \frac{\hbar\mathbf{q}}{2}} w_t \int_{-\infty}^t dt' w_{t'} n_{t'} \\ &\times \left\{ \exp\left[i\left(\frac{\varepsilon_{\mathbf{p} + \frac{\hbar\mathbf{q}}{2}}}{\hbar} - \Delta\omega\right)(t' - t)\right] + (c.c., \mathbf{q} \rightarrow -\mathbf{q}) \right\} \end{aligned} \quad (6)$$

and the right-hand side of Eq. (5) is determined through the evolution of  $n_t$ . The solution of (5) takes the form  $f_{\mathbf{p}, \mathbf{q}t} = \int_{-\infty}^t dt' \exp[-i\mathbf{q} \cdot \mathbf{v}(t - t')] G_{\mathbf{p}, \mathbf{q}t'}$ , so the description of the transient evolution is reduced to the calculation of a multiple integral and to the solution of Eq. (4).

A simplified consideration of the problem is possible under the condition  $\Delta\omega\tau_{ex} > 1$  (photoionization into a high-energy state of  $c$ -band) when  $w_{t'} n_{t'}$  in Eqs. (4) and (6) can be replaced by  $w_t n_t$  due to the fast oscillating factors (the local time approximation). The integration over  $dt'$  in Eq. (6), which is performed with an infinitesimal damping factor in the exponent,  $\delta \rightarrow +0$ , gives

$$\begin{aligned} G_{\mathbf{p}, \mathbf{q}t} &\approx \left(\frac{eE v_{cv}}{\hbar\omega}\right)^2 I_{\mathbf{p} + \hbar\mathbf{q}/2} I_{\mathbf{p} - \hbar\mathbf{q}/2} w_t^2 n_t \\ &\times \left[ \frac{\hbar/i}{\varepsilon_{\mathbf{p} + \hbar\mathbf{q}/2} - \hbar\Delta\omega - i\delta} + (c.c., \mathbf{q} \rightarrow -\mathbf{q}) \right]. \end{aligned} \quad (7)$$

Here the kinetic energy of the inhomogeneous system ( $\mathbf{q} \neq 0$ ) is not conserved during the photogeneration process, even for the long  $\tau_{ex}$  case, due to the violation of the momentum conservation law. Using Eq. (7) and performing the Fourier transformation of the distribution

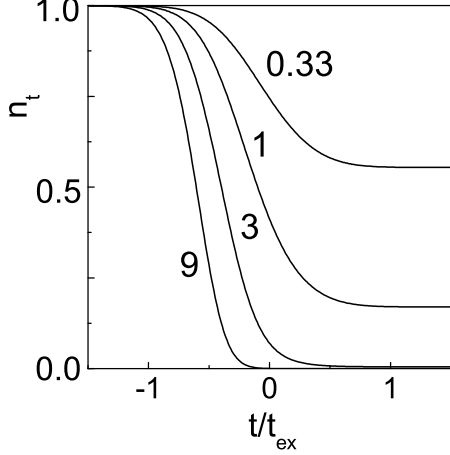


FIG. 1: Transient evolution of the population of short-range level under the dimensionless pumpings  $\gamma\tau_{ex}/2 = 0.33, 1, 3$  and  $9$ .

function  $f_{\mathbf{p},\mathbf{q}t}$  one obtains:

$$f_{\mathbf{p},\mathbf{x}t} = \sum_{\mathbf{q}} \int_{-\infty}^t dt' e^{i\mathbf{q}\cdot\mathbf{x}_{t-t'}} G_{\mathbf{p},\mathbf{q}t'} \\ \approx 2\hbar \left( \frac{eE_{V_{cv}}}{\hbar\omega} \right)^2 \int_{-\infty}^t dt' w_t^2 n_{t'} \sum_{\mathbf{q}} I_{\mathbf{p}+\frac{\hbar\mathbf{q}}{2}} I_{\mathbf{p}-\frac{\hbar\mathbf{q}}{2}} \\ \times \left[ \pi\delta(\varepsilon_{\mathbf{p}+\frac{\hbar\mathbf{q}}{2}} - \hbar\Delta\omega) \cos(\mathbf{q}\cdot\mathbf{x}_{t-t'}) + \frac{\sin(\mathbf{q}\cdot\mathbf{x}_{t-t'})}{\varepsilon_{\mathbf{p}+\frac{\hbar\mathbf{q}}{2}} - \hbar\Delta\omega} \right], \quad (8)$$

where we have introduced the time-dependent coordinate,  $\mathbf{x}_{t-t'} = \mathbf{x} - \mathbf{v}(t-t')$ . The function  $f_{\mathbf{p},\mathbf{x}t}$  satisfies the conditions  $f_{-\mathbf{p},-\mathbf{x}t} = f_{\mathbf{p},\mathbf{x}t}$  and  $f_{-\mathbf{p},\mathbf{x}t} = f_{\mathbf{p},-\mathbf{x}t}$ , which are verified by the exchange  $\mathbf{q} \rightarrow -\mathbf{q}$  in Eq. (8).

Within the local time approximation, Eq. (4) takes the form:

$$\left( \frac{d}{dt} + \gamma w_t^2 \right) n_t = 0, \\ \gamma = 4\pi \left( \frac{eE_{V_{cv}}}{\hbar\omega} \right)^2 \sum_{\mathbf{p}} |I_{\mathbf{p}}|^2 \delta(\varepsilon_{\mathbf{p}}/\hbar - \Delta\omega), \quad (9)$$

where  $\gamma$  stands for the photoionization decrement. The analytical solution of Eq. (9),

$$n_t = 1 - \gamma \int_{-\infty}^t dt' w_t^2 \exp\left(-\gamma \int_{t'}^t dt'' w_t^2\right), \quad (10)$$

describes the transient population of the level [17]. Thus, we have obtained the Wigner distribution (8), and the population (10) written in the integral forms which contain the overlap integral  $I_{\mathbf{p}}$  and the form-factor  $w_t$ .

### III. SHORT-RANGE CASE

To calculate the distribution (8) and the population (10) we use below the overlap integral for the short-range local state with the characteristic size  $l_o$ , so that  $I_{\mathbf{p}} \simeq l_o/L$  if  $p < \hbar/l_o$  and  $I_{\mathbf{p}} \simeq 0$  if  $p > \hbar/l_o$ ; here  $L$  is the normalization length. Within the above assumption, the decrement of photoionization in Eq. (9) takes the form:

$$\gamma \simeq \left( \pi \frac{eE_{V_{cv}}}{\hbar\omega} l_o \right)^2 \hbar \rho_{B2D} = \frac{\pi^3 m}{2m_h} \left( \frac{eE_{V_{cv}}}{\hbar\omega} \right)^2 \frac{\hbar}{\Delta E}, \quad (11)$$

where  $\rho_{B2D}$  is the density of states,  $m_h$  is the heavy hole mass, and the level coupling energy,  $\Delta E$ , is expressed through  $l_o$  according to  $\Delta E \simeq (\hbar/l_o)^2/2m_h$ . The temporal dependencies of  $n_t$  under different pumping level, which is determined by the dimensionless parameter  $\gamma\tau_{ex}/2$ , are shown in Fig. 1 for the Gaussian form-factor  $w_t = \exp[-2(t/\tau_{ex})^2]$ . The complete ionization of the center appears under the condition  $\gamma\tau_{ex}/2 \sim 2$  and, when  $\gamma$  increases, the photoionization takes place during the front of pulse. The full ionization regime takes place under a pulse energy  $\sim 0.2\mu J$  focused on an area  $\sim 100\mu m$ ; this estimate is performed for the GaAs parameters and does not depend on the pulse duration.

Next, we turn to the description of the photoexcited electron distribution given by Eq. (8) and dependent on time,  $|\mathbf{p}|$ ,  $|\mathbf{x}|$ , and the angle  $\widehat{\mathbf{p},\mathbf{x}}$ . We consider the long-duration excitation case (the dynamic regime of response takes place for the nanosecond time scale) and demonstrate that the Wigner distribution  $f_{\mathbf{p},\mathbf{x}t}$  is not a positive-definite function. We calculate below the distribution at the maximal pumping,  $t = 0$ , for the cases  $\mathbf{p}\parallel\mathbf{x}$  and  $\mathbf{p}\perp\mathbf{x}$  with the use of the notations  $f_{p,x}^{\parallel}$  and  $f_{p,x}^{\perp}$ , respectively. Performing in Eq. (8) the integration over  $\mathbf{q}\perp\mathbf{p}$  one obtains the distributions  $f_{p,x}^{\parallel,\perp}$  as follows:

$$\left| \frac{f_{p,x}^{\parallel}}{f_{p,x}^{\perp}} \right| = \frac{2\gamma}{\pi} \int_{-\infty}^0 dt w_t^2 n_t \int_{-\infty}^{\infty} dp_1 \left\{ \frac{\theta[p_{\Delta\omega}^2 - p_1^2]}{\sqrt{p_{\Delta\omega}^2 - p_1^2}} \right. \\ \times \left| \frac{\cos\left[\frac{2(p_1-p)}{\hbar}(x+vt)\right]}{\cos\left[\frac{2x}{\hbar}\sqrt{p_{\Delta\omega}^2 - p_1^2} + \frac{2(p_1-p)}{\hbar}vt\right]} \right| + \frac{\theta[p_1^2 - p_{\Delta\omega}^2]}{\sqrt{p_1^2 - p_{\Delta\omega}^2}} \\ \times \left. \left| \frac{\sin\left[\frac{2(p_1-p)}{\hbar}(x+vt)\right]}{\exp\left[-\frac{2x}{\hbar}\sqrt{p_1^2 - p_{\Delta\omega}^2}\right] \sin\left[\frac{2(p_1-p)}{\hbar}vt\right]} \right| \right\} \quad (12)$$

where  $\theta[z]$  is the Heaviside step function,  $v = |\mathbf{v}|$ , and  $p_{\Delta\omega} = \sqrt{2m\hbar\Delta\omega}$  is the characteristic momentum. The integrals over  $t$  and  $p_1$  can be factorized for the slow electron case,  $p \simeq 0$ ; moreover, a non-zero contribution appears from the first addendum only. The distributions for the  $\parallel$  and  $\perp$  orientations are coincident,

$$f_{p=0,x}^{\parallel,\perp} \simeq 2\gamma \int_{-\infty}^0 dt w_t^2 n_t J_0\left(\frac{2p_{\Delta\omega}x}{\hbar}\right), \quad (13)$$

and the coordinate dependence is given by the zero-order Bessel function,  $J_0(z)$ , which has an alternating-sign value and decreases as a square root.

The distribution functions (12) depend on the dimensionless momentum and coordinate,  $p/p_{\Delta\omega}$  and  $xp_{\Delta\omega}/\hbar$ , the detuning parameter,  $\Delta\omega\tau_{ex}$ , and the pumping intensity,  $\gamma$ . Using (10) with the dimensionless pumping  $\gamma\tau_{ex}/2 = 3$  and performing the numerical integration in Eq. (12) we plot the Wigner distribution for  $\Delta\omega\tau_{ex} = 10$  as it is shown in Fig. 2. One can see a non-monotonically dependency on  $p/p_{\Delta\omega}$  and  $xp_{\Delta\omega}/\hbar$  with pronounced negative contributions. Both longitudinal and transverse cases show a fast decrease with dimensionless momentum, whereas oscillations slowly decrease with dimensionless coordinate due to the spread of the distribution under propagation.

#### IV. MEAN VALUES

The transient dynamics of the Wigner distribution under consideration can be verified by the treatment of spatio-temporal dependencies of the mean values (concentration, energy, and flow,  $n_{xt}$ ,  $\mathcal{E}_{xt}$ , and  $\mathbf{i}_{xt}$ ) given by the standard formulas:

$$\begin{vmatrix} n_{xt} \\ \mathcal{E}_{xt} \\ \mathbf{i}_{xt} \end{vmatrix} = 2 \int \frac{d\mathbf{p}}{(2\pi\hbar)^2} \begin{vmatrix} 1 \\ \varepsilon_p \\ \mathbf{v} \end{vmatrix} f_{\mathbf{p}xt}. \quad (14)$$

Below we analyze the spatio-temporal evolution of (14) using the distribution (8). Performing the integration over the variable  $\mathbf{p} \pm \hbar\mathbf{q}/2$  one obtains the concentration and energy distributions, which are isotropic over the  $\mathbf{x}$ -plane:

$$\begin{vmatrix} n_{xt} \\ \mathcal{E}_{xt} \end{vmatrix} = \frac{\gamma}{2\pi} \int_{-\infty}^t dt' w_t^2 n_{t'} \int_0^\infty dq q J_0(qx) \begin{vmatrix} N_{q,t-t'} \\ E_{q,t-t'} \end{vmatrix}. \quad (15)$$

Here the kernels  $N_{q,\tau}$  and  $E_{q,\tau}$  are given by

$$\begin{aligned} N_{q,\tau} &= \cos\left(\frac{\varepsilon\hbar q\tau}{\hbar}\right) J_0(qv_{\Delta\omega}\tau) \\ &+ \sin\left(\frac{\varepsilon\hbar q\tau}{\hbar}\right) \mathcal{P} \int_0^\infty dy \frac{J_0(qv_{\Delta\omega}\tau\sqrt{y})}{\pi(y-1)} \end{aligned} \quad (16)$$

and

$$\begin{aligned} E_{q,\tau} &= \cos\left(\frac{\varepsilon\hbar q\tau}{\hbar}\right) \left(\hbar\Delta\omega + \frac{\varepsilon\hbar q}{4}\right) J_0(qv_{\Delta\omega}\tau) \\ &+ \sin\left(\frac{\varepsilon\hbar q\tau}{\hbar}\right) \mathcal{P} \int_0^\infty dy \left(\hbar\Delta\omega y + \frac{\varepsilon\hbar q}{4}\right) \frac{J_0(qv_{\Delta\omega}\tau\sqrt{y})}{\pi(y-1)} \\ &+ \hbar q v_{\Delta\omega} \left[ \cos\left(\frac{\varepsilon\hbar q\tau}{\hbar}\right) \mathcal{P} \int_0^\infty dy \sqrt{y} \frac{J_1(qv_{\Delta\omega}\tau\sqrt{y})}{\pi(y-1)} \right. \\ &\quad \left. - \sin\left(\frac{\varepsilon\hbar q\tau}{\hbar}\right) J_1(qv_{\Delta\omega}\tau) \right] \end{aligned} \quad (17)$$

where  $\mathcal{P}$  means the principal value of the integral,  $J_1(z)$  is the first-order Bessel function,  $v_{\Delta\omega} \equiv p_{\Delta\omega}/m$ , and  $y = \varepsilon/\hbar\Delta\omega$  is the dimensionless energy. The distributions (15) depend on the pumping intensity through  $n_t$ , given by Eq. (10), and on the dimensionless coordinate and time,  $xp_{\Delta\omega}/\hbar$  and  $t/\tau_{ex}$ .

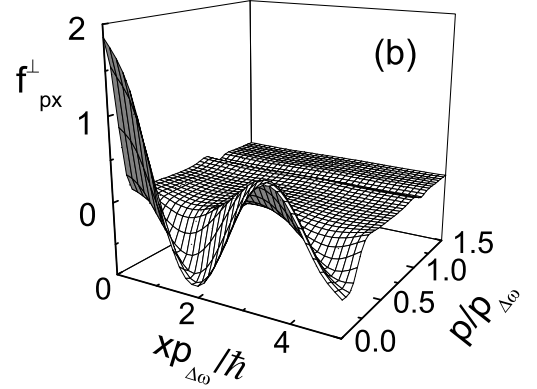
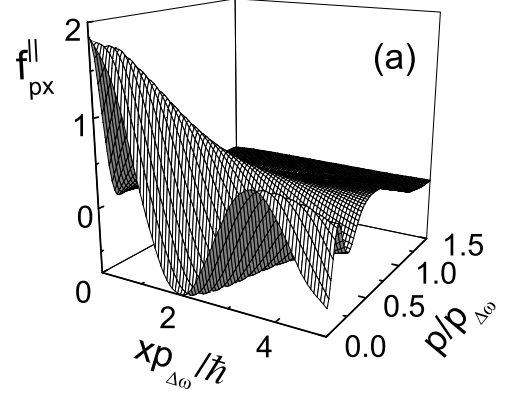


FIG. 2: Longitudinal (a) and transverse (b) Wigner distributions at maximal pumping ( $t = 0$ ) versus dimensionless momentum and coordinate,  $p/p_{\Delta\omega}$  and  $xp_{\Delta\omega}/\hbar$ .

Before numerical calculations, we consider the asymptotes of  $n_{xt}$  (similar formulas can be written for  $\mathcal{E}_{xt}$  and the flow distribution) for the case  $t \gg \tau_{ex}$  and  $x \gg \hbar/p_{\Delta\omega}$ . Using the asymptotic expansion of the Bessel function for large arguments and performing the integrations over  $t'$  and  $q$ , one obtains the explicit ex-

pression

$$n_{xt} = \frac{\gamma\tau_{ex}\mathcal{N}}{(2\pi)^2 l_{\Delta\omega}\sqrt{xv_{\Delta\omega}t}} \sqrt{\frac{\pi}{\Delta\omega t}} \left\{ \sin\left(z_-^2 + \frac{\pi}{4}\right) - \sin\left(z_+^2 + \frac{\pi}{4}\right) + \mathcal{P} \int_0^\infty \frac{dy}{\pi\sqrt{y}(y-1)} \times \left[ \cos\left(z_{y-}^2 + \frac{\pi}{4}\right) - \sin\left(z_{y+}^2 + \frac{\pi}{4}\right) \right] \right\}, \quad (18)$$

where  $\mathcal{N} = \int_{-\infty}^\infty dt w_t^2 n_t / \tau_{ex}$ ,  $l_{\Delta\omega} = \hbar/p_{\Delta\omega}$ , and we have introduced the dimensionless forms  $z_\pm = (x \pm v_{\Delta\omega}t)p_{\Delta\omega}/2\hbar\sqrt{\Delta\omega t}$  and  $z_{y\pm} = z_\pm \pm (\sqrt{y}-1)\sqrt{\Delta\omega t}$ . Thus, the period of oscillations of the concentration distribution,  $(\hbar/2p_{\Delta\omega})\sqrt{\Delta\omega t}$ , does not depend on  $\Delta\omega$  and increases as  $\sqrt{t}$ .

The spatio-temporal dependency of the concentration is shown in Figs. 3. Fig. 3(a) shows the 3D graph near the peak at  $xp_{\Delta\omega}/\hbar = 0$  for  $\Delta\omega\tau_{ex} = 5$  and  $\gamma\tau_{ex}/2 = 1$ . As can be seen, concentration falls quickly for small dimensionless coordinate and oscillates for bigger  $xp_{\Delta\omega}/\hbar$  values. At the same time maximum position in dimensionless time is shifted following the classical velocity as shown in Fig. 3(b) where the contour plot together with the line corresponding to the classical velocity is presented. Concentration is normalized by  $n_0 = \gamma\tau_{ex}m\Delta\omega/\pi\hbar$ , which is equal to  $2.82 \times 10^{11} \text{ cm}^{-2}$  for  $\hbar\Delta\omega = 5 \text{ meV}$ , and  $\gamma\tau_{ex}/2 = 1$ . This value corresponds to an excited electron localized over an area of the order of  $(\hbar/p_{\Delta\omega})^2$ .

Fig. 4 shows the behavior of the energy distribution vs. dimensionless position and time. Energy distribution has been normalized by  $E_0 = n_0\hbar\Delta\omega$ , which corresponds to  $2.25 \times 10^{-3} \text{ erg/cm}^2$  for the same values of  $\hbar\Delta\omega$  and  $\gamma\tau_{ex}/2$  used for the concentration. Energy behavior vs.  $xp_{\Delta\omega}/\hbar$  is similar to the concentration one. To say, a fast decrease followed by oscillations.

Since the in-plane isotropy of the problem, one obtains the flow density:  $\mathbf{i}_{xt} = (\mathbf{x}/|\mathbf{x}|)I_{xt}$ , where the scalar function  $I_{xt}$  takes a similar form to (15):

$$I_{xt} = \frac{\gamma}{2\pi} \int_{-\infty}^t dt' w_t^2 n_{t'} \int_0^\infty dq q J_1(qx) F_{q,t-t'} \quad (19)$$

with the kernel

$$F_{q,\tau} = \frac{\hbar q}{2m} \left[ \cos\left(\frac{\varepsilon\hbar q\tau}{\hbar}\right) \mathcal{P} \int_0^\infty dy \frac{J_0(qv_{\Delta\omega}\tau\sqrt{y})}{\pi(y-1)} - \sin\left(\frac{\varepsilon\hbar q\tau}{\hbar}\right) J_0(qv_{\Delta\omega}\tau) \right] - v_{B\Delta\omega} \left[ \cos\left(\frac{\varepsilon\hbar q\tau}{\hbar}\right) J_1(qv_{\Delta\omega}\tau) - \sin\left(\frac{\varepsilon\hbar q\tau}{\hbar}\right) \mathcal{P} \int_0^\infty \frac{dy\sqrt{y}}{\pi(y-1)} J_1(qv_{\Delta\omega}\tau\sqrt{y}) \right] \quad (20)$$

Performing the numerical integrations given by Eqs. (19, 20) we plot the flow distribution for the above parameters, as it is shown in Fig. 5. Flow distribution has also been normalized by  $I_0 = n_0 p_{\Delta\omega}/m$ , being  $I_0 = 4.57 \times 10^{18} \text{ (cm/s)/cm}^2$  for the above values of  $\hbar\Delta\omega$  and

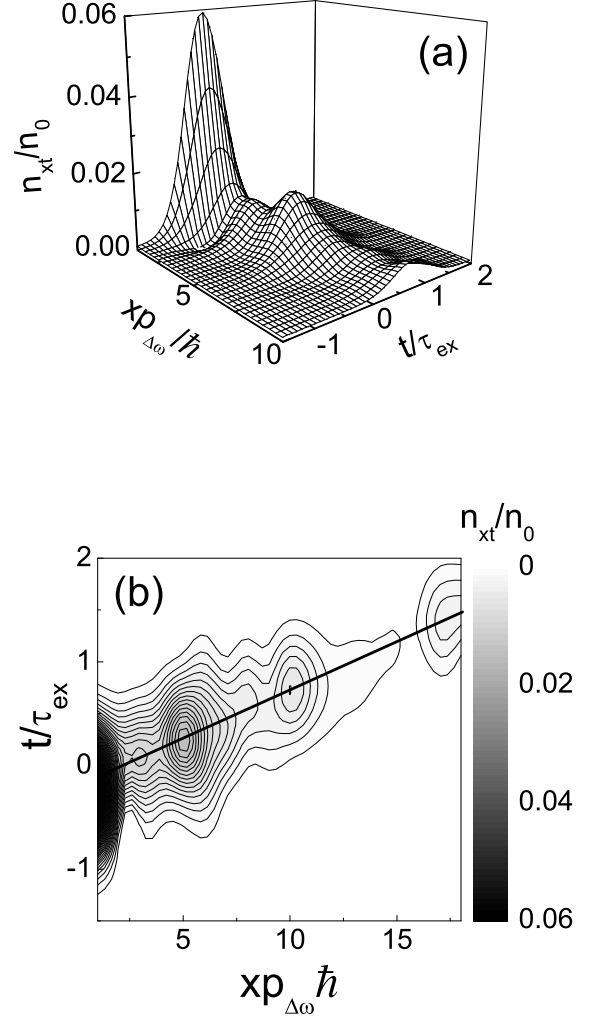


FIG. 3: Spatio-temporal evolution of concentration,  $n_{xt}$ , for  $\gamma\tau_{ex}/2 = 1$ . (a) 3D graph near the peak, and (b) contour plot showing the line corresponding to the classical velocity.

$\gamma\tau_{ex}/2$ . Once again it appears an initial fast decrease, followed by oscillations in dimensionless coordinate. Moreover, as can be seen, there are oscillations also in time and negative values of the flow distribution arise.

## V. CONCLUSIONS

In summary, we have suggested a new scheme to investigate the quantum peculiarities of the single-particle dynamics under ultrafast photoionization of a single deep

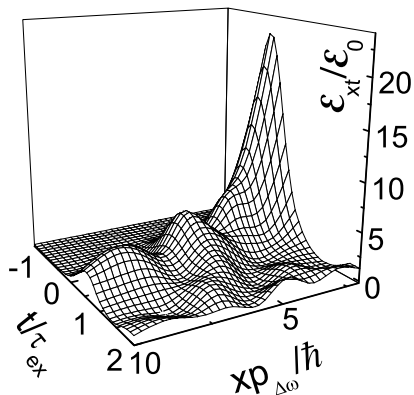


FIG. 4: Evolution of energy,  $\mathcal{E}_{xt}$ , for the same parameters of Fig. 3.

impurity. Due to the negative contributions to transient Wigner distribution of  $c$ -band electron, the mean concentration, energy, and flow demonstrate an oscillatory behavior in contrast to the classical results (see Appendix). We have analyzed the conditions for visible quantum oscillations, when a direct experimental mapping of the quantum distribution should be possible.

Now we turn to the discussion of possibilities for experimental verification of the peculiarities obtained. The stage of selective single-electron photoexcitation is based on the assumption of a low concentration of deep impurities: if a bulk concentration less than  $10^{12}\text{cm}^{-3}$  remains in the near-surface region, one obtains an inter-center distance about  $1\mu\text{m}$ . The regime of a single-center excitation can be easily realized with an ultrafast pump focused over a submicron scale. Recently, similar measurements were performed with a single quantum dot [18] but the photoexcitation into continuum and further evolution of distribution was not examined. Perhaps, it is due to the complicate problem of the registration of the oscillating Wigner distribution. In spite of the sensitive optical methods developed recently for optical control of a single quantum dot (see [19, 20] and Refs. therein) the spatial resolution remains a complicate task (we use above  $\hbar/p_{\Delta\omega} \sim 10\text{ nm}$ ). Note that the period of the oscillations increases with time as  $\sqrt{t}$  [see Eq. (18) and Fig. 3b] but the distribution value (and the response) decreases due to spatial spread. Another possibility is to use the scanning tunneling microscopy [21] which has nanometer resolution but has to be adapted to time-resolved measurements with subnanosecond resolution. Note, that we do

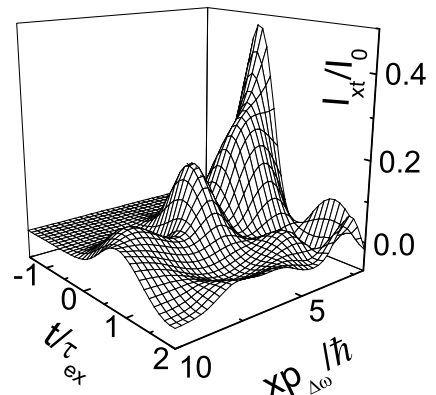


FIG. 5: Evolution of the flow,  $I_{xt}$ , for the same parameters of Fig. 3.

not calculate any concrete optical or tunneling response supposing that the observed peculiarities will be of the same order as the mean values considered in Sec. IV.

Next, we discuss the assumptions used in our calculations. The main approximation is the local time approach, so that the edge photoexcitation is beyond of our consideration. A more complicate numerical simulation is required for this case as well as to take into account the Coulomb correlations (excitonic effect). The interaction of the electron with the localized hole is essential for a near-center region but it should decrease with  $x$ . Thus, the short-range model used in our calculations of Eqs. (9, 11) is enough in order to estimate the photoionization decrement. Finally, only the averaged Wigner distribution has been considered and a full counting statistics of photoionization and subsequent transient propagation of electrons [21] requires a special investigation.

In closing, a similar theoretical analysis may be developed for other cases like photoexcitation of a single quantum dot or near-field photoexcitation [14, 18], where a similar quantum behavior should take place. We hope that these results will stimulate experimental efforts towards a mapping of quantum peculiarities in the transient Wigner distribution.

#### APPENDIX A: CLASSICAL EVOLUTION

This appendix contains the description of the classical regime of transient evolution when the generation rate in

plane scale of excitation, and  $w_t$  is the above-introduced form-factor. After the integration over  $\mathbf{q}$ -plane, the distribution  $f_{\mathbf{p},\mathbf{x}t}$  takes the form:

$$f_{\mathbf{p},\mathbf{x}t} \propto \delta_{\Delta\varepsilon}(\varepsilon - \varepsilon_{ex}) \int_{-\infty}^t dt' w_{t'} \exp \left[ -\frac{1}{2} \left( \frac{\mathbf{x}_{t-t'}}{l_{ex}} \right)^2 \right], \quad (\text{A2})$$

so  $f_{\mathbf{p},\mathbf{x}t} > 0$  because of the positive functions under integral. At  $t \gg \tau_{ex}$  one obtains the distribution as a moving Gaussian peak:  $f_{\mathbf{p},\mathbf{x}t} \propto \delta_{\Delta\varepsilon}(\varepsilon - \varepsilon_{ex}) \exp[-(1/2)(\mathbf{x}_t/l_{ex})^2]$ . The explicit expressions for  $f_{\mathbf{p},\mathbf{x}}^{\parallel,\perp}$  introduced in analogy to Eq. (12) can be written through the probability integrals and they have a single-peak behavior.

Restricting ourself to a narrow energy distribution,  $\Delta\varepsilon \ll \varepsilon_{ex}$ , and taking the integrals over  $\mathbf{p}$ -plane according the definition (14), one obtains the concentration distribution as follows:

$$n_{xt} \propto \exp \left[ -\frac{1}{2} \left( \frac{x}{l_{ex}} \right)^2 \right] \int_{-\infty}^{t/\tau_{ex}} d\tau e^{-2\tau^2} \times e^{-\alpha(t/\tau_{ex}-\tau)^2} I_0 \left[ \alpha \frac{x}{l_{ex}} \left( \frac{t}{\tau_{ex}} - \tau \right) \right], \quad (\text{A3})$$

where  $I_0(z)$  is the zero-order Bessel function of imaginary argument. Here we have introduced the dimensionless parameter  $\alpha = v_{ex}\tau_{ex}/l_{ex}$  with  $v_{ex} = \sqrt{2\varepsilon_{ex}/m}$ . Within the above approximation, the energy distribution is given by  $\mathcal{E}_{xt} \simeq \varepsilon_{ex}n_{xt}$ . Similar to Eqs. (19, 20) one obtains the flow density  $\mathbf{i}_{\mathbf{x}t} = (\mathbf{x}/|\mathbf{x}|)I_{xt}$ , where the scalar function  $I_{xt}$  is written as follows:

$$I_{xt} \propto v_{ex} \exp \left[ -\frac{1}{2} \left( \frac{x}{l_{ex}} \right)^2 \right] \int_{-\infty}^{t/\tau_{ex}} d\tau e^{-2\tau^2} e^{-\alpha(t/\tau_{ex}-\tau)^2} I_1 \left[ \alpha \frac{x}{l_{ex}} \left( \frac{t}{\tau_{ex}} - \tau \right) \right]. \quad (\text{A4})$$

where  $I_1(z)$  is the first-order Bessel function of imaginary argument.

Performing a simple numerical integration of Eqs. (A3) and (A4) one obtains the concentration and flow distributions versus the dimensionless coordinate and time,  $x/l_{ex}$  and  $t/\tau_{ex}$ , as it is shown in Fig. 6 for  $\alpha = 6$ . Since there are no oscillation of the classical distribution (A2), the mean values appear to be spread monotonically.

## ACKNOWLEDGMENTS

This work has been supported in part by Ministerio de Educación y Ciencia (Spain) and FEDER under the project FIS2005-01672, and by FRSF of Ukraine (grant No.16/2).

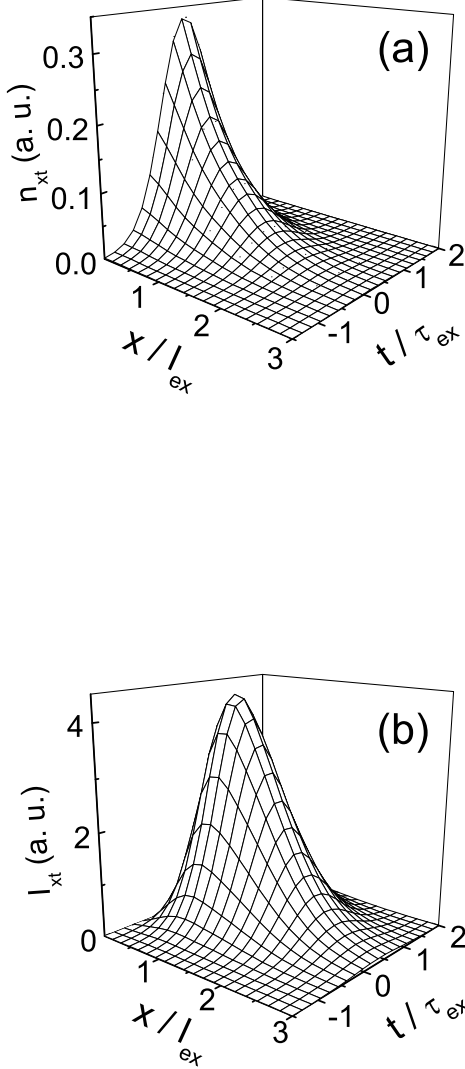


FIG. 6: Evolution of the classical distributions  $n_{xt}$  (a) and  $I_{xt}$  given by Eqs. (A3) and (A4) for  $\alpha = 6$ .

Eq. (8) is approximated by the factorized expression:

$$G_{\mathbf{p},\mathbf{q}t} \propto \delta_{\Delta\varepsilon}(\varepsilon - \varepsilon_{ex}) e^{-(ql_{ex})^2} w_t. \quad (\text{A1})$$

Here  $\delta_{\Delta\varepsilon}(\varepsilon - \varepsilon_{ex})$  is the peak energy distribution with the half-width  $\Delta\varepsilon$  placed at the energy  $\varepsilon_{ex}$ ,  $l_{ex}$  is the in-

- [1] M. Shapiro, P. Brumer, *Physics Reports*, **425**, 195 (2006); W.S. Warren, H. Rabitz, M. Dahleh, *Science* **259**, 1581 (1993).
- [2] J. Shah, *Ultrafast Spectroscopy of Semiconductors and Semiconductor Nanostructures* (Springer, Heidelberg, 1999).
- [3] *Nonequilibrium Physics at Short Time Scales*, Ed. by K. Morawetz (Springer, Heidelberg, 2004), part III.
- [4] V.M. Axt and T. Kuhn, *Rep. Prog. Phys.* **67**, 433 (2004).
- [5] M. Nedjalkov, D. Vasileska, D.K. Ferry, C. Jacoboni, C. Ringhofer, I. Dimov, and V. Palankovski, *Phys. Rev. B* **74**, 035311 (2006); M. Nedjalkov, H. Kosina, S. Selberherr, C. Ringhofer, and D.K. Ferry, *Phys. Rev. B* **70**, 115319 (2004).
- [6] P. Lazic, V.M. Silkin, E.V. Chulkov, P.M. Echenique, and B. Gumhalter, *Phys. Rev. Lett.* **97**, 086801 (2006); B. Gumhalter, *Phys. Rev. B* **72**, 165406 (2005).
- [7] R. Huber, F. Tauser, A. Brodschelm, M. Bichler, G. Abstreiter, and A. Leitenstorfer, *Nature* **414**, 286 (2001).
- [8] R.A. Kaindl, M.A. Carnahan, D. Hagele, R. Lovenich, and D.S. Chemla, *Nature* **423**, 734 (2003).
- [9] M. Hase, M. Kitajima, A.M. Constantinescu, and H. Petek, *Nature* **426**, 51 (2003).
- [10] R. Huber, C. Kübler, S. Tübel, A. Leitenstorfer, Q. T. Vu, H. Haug, F. Köhler, and M.-C. Amann, *Phys. Rev. Lett.* **94**, 027401 (2005).
- [11] M. Herbst, M. Glanemann, V. M. Axt, and T. Kuhn, *Phys. Rev. B* **67**, 195305 (2003); T. Wolterink, V. M. Axt, and T. Kuhn, *Phys. Rev. B* **67**, 115311 (2003).
- [12] F.T. Vasko and O.E. Raichev, *Quantum Kinetic Theory and Applications* (Springer, New York, 2005).
- [13] P.J. Burke, I.B. Spielman, J.P. Eisenstein, L.N. Pfeiffer and K. W. West, *Appl. Phys. Lett.* **76**, 745 (2000).
- [14] U. Neuberth, L. Walter, G. von Freymann, B. DalDon, H. Kalt, M. Wegener, G. Khitrova, and H. M. Gibbs, *Appl. Phys. Lett.* **80**, 3340 (2002); Y. Yayon, A. Esser, M. Rappaport, V. Umansky, H. Shtrikman, and I. Bar-Joseph, *Phys. Rev. Lett.* **89**, 157402 (2002); T. Guenther, V. Emiliani, F. Intonti, C. Lienau, T. Elsaesser, R. Nötzel and K. H. Ploog, *Appl. Phys. Lett.* **75**, 3500 (1999).
- [15] N.M. Kolchanova, I.D. Loginova, and I.N. Yassievich, *Fiz. Tv. Tela* **25**, 1650 (1983) [*Sov. Phys. - Solid State* **25**, 952 (1983)]; N.M. Kolchanova, M.A. Sipovskaya, Y.S. Smetannikova, *Sov. Phys. Semicond.* **16**, 1418 (1982).
- [16] V.I. Perel and I.N. Yassievich, *Sov. Phys. - JETP* **55**, 143 (1982) [*Zh. Eksp. Teor. Fiz.* **87**, 237 (1982)].
- [17] Note, that the particle conservation law,
- $$\frac{d}{dt} \left( 2 \sum_{\mathbf{p}} f_{\mathbf{p}, \mathbf{q}=0t} + n_t \right) = 0,$$
- can be verified under calculation of the time derivative of  $2 \sum_{\mathbf{p}} f_{\mathbf{p}, \mathbf{q}=0t}$  with the use of Eqs. (8, 9).
- [18] T. Guenther, C. Lienau, T. Elsaesser, M. Glanemann, V. M. Axt, T. Kuhn, S. Eshlaghi and A. D. Wieck, *Phys. Rev. Lett.* **89**, 057401 (2002); M. Wesseli, C. Ruppert, S. Trumm, H. J. Krenner, J. J. Finley, and M. Betz, *Appl. Phys. Lett.* **88**, 203110 (2006).
- [19] Q.Q. Wang, A. Muller, P. Bianucci, C. K. Shih, M. T. Cheng, H. J. Zhou, and J. B. Han, *Appl. Phys. Lett.* **89**, 142112 (2006); Y. Wu, X. Li, L.M. Duan, D.G. Steel, and D. Gammon, *Phys. Rev. Lett.* **96**, 087402 (2006).
- [20] S. Seidl, A. Högele, M. Kroner, K. Karrai, R. J. Warburton, J. M. Garcia, and P. M. Petroff, *Phys. Stat. Sol. (a)* **204**, 381 (2007); P. A. Dalgarno, J. McFarlane, B. D. Gerardot, R. J. Warburton, K. Karrai, A. Badolato, and P. M. Petroff, *Appl. Phys. Lett.* **89**, 043107 (2006).
- [21] A.M. Yakunin, A.Yu. Silov, P.M. Koenraad, J.H. Wolter, W. Van Roy, J. De Boeck, J.-M. Tang and M.E. Flatte, *Phys. Rev. Lett.* **92**, 216806 (2004); G. Mahieu, B. Grandidier, D. Deresmes, J. P. Nys, D. Stievenard, and Ph. Ebert, *Phys. Rev. Lett.* **94**, 026407 (2005).
- [22] T. Fujisawa, T. Hayashi, S. Sasaki, *Rep. on Progress in Physics* **69**, 759 (2006); D.A. Bagrets, Y. Utsumi, D.S. Golubev, G. Schon, *Fortschr. Phys. (Progress of Physics)* **54**, 917 (2006).